Engineering Science and Technology, an International Journal 23 (2020) 576–584

HOSTED BY

Contents lists available at ScienceDirect

Engineering Science and Technology, an International Journal

journal homepage: www.elsevier.com/locate/jestch

Full Length Article

Modelling and voltage control of the solar-wind hybrid micro-grid with optimized STATCOM using GA and BFA

Hale Bakir, Ahmet Afsin Kulaksiz *

Department of Electrical & Electronics Engineering, Konya Technical University, Konya, Turkey

A R T I C L E I N F O

Article history:
Received 26 April 2019
Revised 1 July 2019
Accepted 30 July 2019
Available online 8 August 2019

Keywords:
Voltage control
Bacteria foraging algorithm
PV-wind hybrid system
Static synchronous compensator
Genetic algorithm

A B S T R A C T

Electricity generation from the wind and solar photovoltaic (PV) systems are highly dependent upon weather conditions. Their intermittent nature leads to fluctuations in their output. Therefore, the need for rapid compensation for energy transmission and distribution systems is increasingly important. Static Synchronous Compensator (STATCOM) can be adopted for reactive power compensation and for decreasing the voltage fluctuation caused by the system and renewable energy sources. This study presents modelling of a Solar PV-Wind Hybrid Micro-grid and the increase of the stable operating limit of the system in case of the incorporation of STATCOM is examined. The major contribution of this paper is the optimization of gain parameters of four PI controllers in STATCOM control circuit based on genetic algorithms (GA) and Bacteria Foraging Algorithm (BFA) and therefore obtaining better responses and voltage stability in terms of nonlinear nature of solar-wind hybrid micro-grid. The Simulink models of the system architecture include a wind turbine model, a solar PV power system model and a STATCOM. It is certified that the voltage fluctuation at the end of the bus bar is reduced by 8% using conventional PI controller, by 10% for GA-based PI controller, and by 15% for BFA based PI controller under variable load. The results obtained by GA and BFA-based optimization of PI controllers are compared with that of the conventional controller and better results attained.

1. Introduction

The applications of renewable energy sources have shown increasing momentum, especially in recent years. Increasing energy consumption, rapid progress in energy production technologies and increasing public awareness for environmental protection lead research areas to alternative energy and distributed production. By using various control techniques, it is possible to create a hybrid structure consisting of an efficient photovoltaic (PV) system and wind energy system for applications with low installed capacity. Since renewable energy systems such as wind alone and hybrid Wind/PV are not completely safe in meeting the demand for the load, power instabilities are experienced and reactive power compensation is an emergent need for stable operation of a hybrid system. Reactive power compensation is a requirement in all energy systems. Reactive power causes concerns involved with different power quality problems as well as increasing power losses. To solve this, the synchronous condensers and fixed mechanical switching capacitors have been used for many years. Compensations of this type have some disadvantages such as large dimensions, high losses and slow response time.

For diminishing power quality problems, improving system stability and for increased power transfer capability, the Flexible Alternating Current Transmission Systems (FACTS) devices have been commercially introduced in the late 1980s [1]. However, new FACTS topologies are emerging to enhance the security and stabilization of micro-grids [2,3]. As a member of FACTS family devices, STATCOM is a shunt-connected inverter-based device that improves power quality in alternating current systems. In 1991, the first installation of the STATCOM was in Japan. It provided voltage stabilization at ±80 MVAR [1]. Since then, the development of real-time controllers has allowed the implementation of complex control algorithms [4]. The role of these devices is power factor improvement, load balancing, voltage regulation and harmonic elimination in energy systems. By increasing the capacity of transmission lines, the need to build new lines are eliminated. Various control strategies are used to allow power system operation within the required operating limits. The most commonly employed controllers are Proportional-Integral (PI), Proportional-Integral-Deriva

* Corresponding author at: Konya Technical University, Faculty of Engineering and Natural Sciences, Department of Electrical and Electronics Engineering, 42250 Selcuklu, Konya, Turkey.

E-mail address: aakulaksiz@ktun.edu.tr (A.A. Kulaksiz).

Peer review under responsibility of Karabuk University.

https://doi.org/10.1016/j.jestch.2019.07.009
2215-0986/© 2019 Karabuk University. Publishing services by Elsevier B.V.

Nomenclature

V_{bus}	grid voltage	w	weighting factor
Q	reactive power	I_{ph}	light generated current
I_a, I_b, I_c	three-phase current components	k	Boltzmann gas constant
V_d, V_q	voltage components	q	electron charge
I_q, I_d	current components	T	absolute temperature
V_w	average wind speed on the area swept by the blades	n	linearity factor
P_w	power produced by the wind turbine	R_s	cell series resistance
T_t	amount of aerodynamic torque	R_{sh}	cell shunt resistance
∂	wind turbine end velocity ratio	N_s	number of PV module in series
C_p	power coefficient	V	output voltage of solar cell
β	angle of inclination	I_0	dark saturation current value
k	constant for wind	I	PV current
R	length of the blades (radius of the turbine rotor)	$V_{statcom}$	output voltage of the STATCOM
C_t	coefficient of torque	V_{ac}	AC system voltage
ρ	air density	α	phase difference between voltages
Ω_t	angular speed of the rotor	x	equivalent reactance of transformers
A	swept area	P	active power
V_a, V_b, V_c	three-phase voltage components	m_a	modulation index
K_p	proportional gain constant	V_{dc}	DC voltage
K_i	integral gain constant	delta (n, i)	direction to represent a tumble
N_s	number of swimming bacteria	N_c	chemotactic steps
i	bacterial index	N_{re}	number of breeding steps
J	performance criterion for optimization	N_{ed}	number of elimination and dispersal steps

tive (PID), Fuzzy Logic Controller (FLC) and Artificial Neural Networks (ANN)-based controllers. In commercial STATCOM devices, generally, conventional PI type controllers are incorporated and the effectiveness of the controller determines the performance of STATCOM. Thereby, the current research is focused on obtaining a more robust and adaptable operation of STATCOM for variations of the hybrid power system.

In recent years, various researches on STATCOM have been made. In 2010, a research was carried out on a hybrid PV-Wind supply system with STATCOM interface for a water-lift station and voltage fluctuation was reduced in a limited manner [5]. In literature, some studies have discussed the stability effect of FACTS controllers on power systems connected to wind system based doubly fed induction generators and focused on the results of rotor angle responses [6].

A control method for Voltage Source Control (VSC)-based STATCOM that uses conventional and direct-current vector control strategies have been proposed. But it only worked on the voltage fluctuation from the system and they did not deal with a hybrid system [7]. Voltage control through reactive power support for wind energy conversion system based hybrid power system has been reported in [8]. But the work did not use STATCOM to reduce the voltage fluctuation with the load side converter. The literature review shows that there is very little research on the STATCOM system-based voltage fluctuations caused by the hybrid solar-wind microgrid. With the increasing installation of PV and wind power systems, the conventional FACTS devices still need improvements by optimizations of controllers and extensive analysis has to be made under various operating conditions. Dynamic analysis of hybrid power systems was made by adjusting the optimum gain of STATCOM in [9]. In another research dealing with a control system using Static Var Compensator (SVC) and Automatic Voltage Regulator (AVR), GA is used to simultaneously determine PI control parameters of SVC and AVR [10]. A searcher optimization algorithm was performed for the isolated hybrid power system model and performance analysis with Takagi-Sugeno type fuzzy logic based controller was reported in [11].

In this study, the objective is to increase the reliable operating limit of the presented power system architecture by incorporating STATCOM for reactive power compensation. Also, it is aimed to reduce the voltage fluctuation occurring due to the varying nature of renewable energy sources.

Optimal adjustment of PI parameters in STATCOM is automatically made based on GA and BFA to get a satisfactory response. The optimization of the PI controller parameters in STATCOM control circuit is performed. To the best knowledge of the authors, a study dealing with the optimization and adjustment methods of four PI controllers in the STATCOM's control circuit for voltage stability of the PV-Wind hybrid system has not been published.

2. Methods

2.1. Wind power system modelling

Today, Doubly Fed Induction Generator (DFIG) is among the most preferred wind generators [12]. DFIG is composed of stator windings that are connected directly to a fixed frequency 3-phase network and back-to-back voltage-based converters placed in rotor windings. The term doubly-fed indicates that the stator voltage is derived from the mains and the rotor voltage is induced by the power converter. The system allows for large but limited variable speeds (can operate with a speed difference of ±40%). The transducers make the mechanical and electrical frequency adjustment by injecting current at different frequencies to the rotor. Generator behavior is managed by power converters or controllers in normal operation or fault conditions [13].

The DFIG consists of successive voltage-induced converters, which are connected directly to the fixed-frequency three-phase grid and are bi-directionally connected to the rotor windings. The main idea is to control the rotor current components of the rectifier on the rotor side and regulate the active and reactive powers. The inverter on the grid side also controls the DC link voltage.

DFIG has many advantages such as the controlling capability of active and reactive power by rotor current [13]. It has two successive converters as rotor side control and grid side control in Fig. 1. In the grid side control circuit of the wind, V_{bus} (grid voltage), Q (reactive power component), three-phase current components (I_a, I_b, I_c) are taken in the grid side control circuit of the wind and V_{bus} and I_d & I_q are regulated. With space vector transformations, voltage components (V_d & V_q) and current components (I_q & I_d) are converted to three-phase signals. The angles are determined with Phase Locked Loop (PLL) by using voltage values and used in Park and Clarke space vector transformation.

The control circuit is implemented in Simulink environment. The aerodynamic model presents the rotor power by computing the mechanical torque determined by air-flow on the blades [14]. Wind speed (V_w) is regarded as the average speed on the area swept by the blades.

The power equation produced by the wind turbine is given in Eq. (1).

$$P_w = \frac{1}{2} C_p \rho A {V_w}^3, \tag{1}$$

The amount of aerodynamic torque in Nm is given in Eq. (2).

$$T_t = \frac{1}{2} \rho R^3 {V_w}^2 C_t, \tag{2}$$

Wind turbine end velocity ratio is given in Eq. (3).

$$\partial = R\Omega_t / V_w, \tag{3}$$

Power coefficient (C_p) adopted as 0.44 refers to the analytical expression as a function of the angle of inclination (β) and the turbine end velocity ratio (∂), k is a constant, R is length of the blades in m (radius of the turbine rotor), C_t is the coefficient of torque, A is the swept area, ρ is the air density (1.225 kg/m^3), Ω_t is the angular speed of the rotor.

The power factor equation is given in Eqs. (4) and (5) [14].

$$C_p = k1\left(\frac{k2}{\partial i} - k3\beta - k4\beta^{k5} - k6\right)\left(\frac{e^{\left(\frac{k7}{\partial i}\right)}}{1}\right), \tag{4}$$

$$\partial i = 1/(\partial + k8), \tag{5}$$

Based on these equations, the characteristics in Fig. 2 are obtained. As can be seen from the figure, if the wind speed is 12 m/s, the output power reaches 2 MW. According to these power and torque equations, a wind turbine model is formed and indirect speed control is modeled to determine the maximum power point. Some data for the Doubly Fed Induction Machine were adopted and a DFIG was modelled [14].

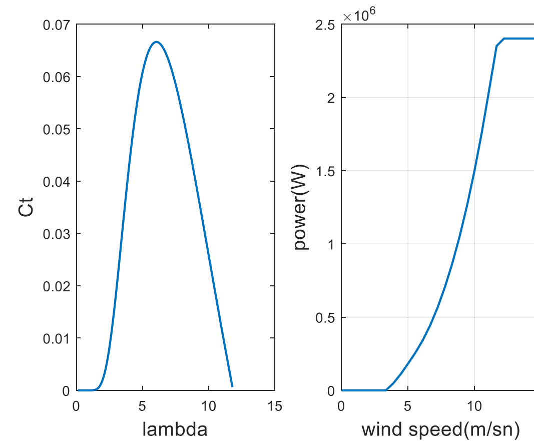

Fig. 2. Characteristics of wind turbine (a) λ-Ct characteristic (b) Velocity- Power (v-P) characteristics.

2.2. Photovoltaic power system modeling

Solar PV panels ensure the generation of electricity in DC form by converting the energy in the sun's rays. In order to increase the power output, many solar cells are connected in parallel or in series and mounted on a surface forming a solar cell module or a photovoltaic module. The PV cells are modelled using the one-diode equivalent circuit. The PV current can be determined as shown in Eq. (6) [15].

$$I = I_{ph} - I_0\left[e^{(V+IR_s)*\frac{q}{nkTN_s}} - 1\right] - \frac{(V+IR_s)}{R_{sh}}, \tag{6}$$

In this statements, I_{ph} is the light generated current, k is Boltzmann gas constant (1.38×10^{-23} J/K), q is electron charge (1.6×10^{-19} C), T is absolute temperature (*Kelvin*), n is linearity fac-

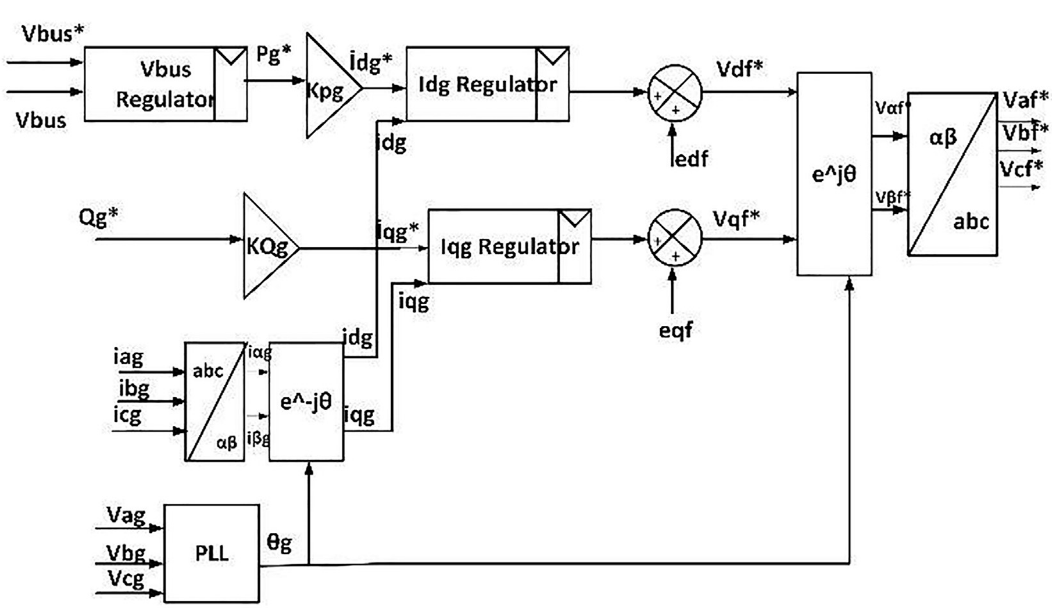

Fig. 1. Grid side control circuit.

tor, R_s is the cell series resistance, R_{sh} is the cell shunt resistance, N_s is the number of PV modules in series, V is the output voltage of solar cell and I_0 shows the dark saturation current value.

The mathematical model of the photovoltaic system with the equations detailed in [15] is implemented in Simulink. In addition, perturbation and observation (P&O) algorithm has been adopted for implementing the maximum power point tracking (MPPT) in PV power system.

2.3. Static synchronous compensator

STATCOM is established from a voltage source DC/AC converter. It provides voltage support by generating or absorbing reactive power at the point of common coupling without the need of large external or capacitor banks [16]. At the STATCOM output, balanced three-phase voltages are obtained at the mains frequency having a controlled amplitude and phase angle. In this embodiment, the power change between the AC system and the device in steady-state is generally reactive. The reactive power change between the AC system and the STATCOM is controlled by controlling the magnitude and phase angle of the transformer output voltage. For this, the magnitude and frequency of the AC output voltage of the inverter in the STATCOM circuit must be set. If the magnitude of the output voltage of the STATCOM exceeds that of the AC system voltage ($V_{statcom} > V_{ac}$), the current flow direction is from the STATCOM to the AC system via transformer reactance and the device supplies reactive power to the transmission line.

In case the STATCOM output voltage is bigger than the transmission line voltage, the device operates in capacitive mode. The capacitor is used to provide the DC voltage required for the inverter. The capacitor is either charged or discharged depending on the phase difference between the output voltage of inverter and the AC system voltage. The active power flowing from the AC system to the STATCOM by neglecting the transformer resistance can be found in Eq. (7) [17];

$$P = \frac{V_{ac}V_{statcom}\sin\alpha}{X}, \tag{7}$$

If $\alpha > 0$, the inverter output voltage is in the same phase as the system voltage. The capacitor is charged because of $P > 0$. If $\alpha < 0$, the capacitor is discharged because of $P < 0$. Reactive power flowing from STATCOM to AC system or from AC system to STATCOM can be calculated by Eq. (8).

$$Q = \frac{V_{ac}V_{statcom}\cos\alpha - V_{ac}^{\,2}}{X}, \tag{8}$$

where V_{ac} is AC system voltage, $V_{statcom}$ is inverter output voltage, X is equivalent reactance of transformers, α is the phase difference between voltages. In the STATCOM, the voltage V_{dc} is kept constant and the amplitude of the AC output voltage of the inverter is calculated by changing the modulation index (m_a).

The modulation index is usually between $0 < m_a < 1$. In case $m_a = 0.75$; there is no power exchange ($V_{ac} = V_{statcom}$). In case $m_a = 0.65$; STATCOM is in inductive mode ($V_{ac} > V_{statcom}$). In case $m_a = 0.85$; STATCOM is in capacitive mode ($V_{statcom} > V_{ac}$). Inverter output voltage in STATCOM can be calculated as shown in Eqs. (9) and (10).

$$V_{statcom} = V_{ef}\frac{\sqrt{3}}{2}, \tag{9}$$

$$V_{ef} = V_{dc}\frac{m_a}{2}, \tag{10}$$

According to Eqs. (9) and (10), the output voltage of STATCOM is adjusted by keeping the DC voltage constant and changing the m_a value.

STATCOM operates either in the capacitive or inductive mode for reactive power compensation in the system in grid limits and to prevent transmission losses. The control of STATCOM is provided by the power electronics switching elements (IGBT) of the inverter and PWM control technique is used. As shown in Fig. 3, the system is connected directly to the reactors. In Fig. 4, a control circuit belonging to STATCOM is given and AC voltage (V_{bus}), DC voltage (V_{dc}), active and reactive current components (I_d & I_q) are regulated and three-phase signals (V_a, V_b, V_c) using Park and Clarke space vector transformations is converted into rotating axis components V_d and V_q. The controls are provided with the PI controller and STATCOM control circuit using PI, and PLL is modelled in MatLab/Simulink. The parameters employed in STATCOM is listed in Table 1.

The proposed hybrid system architecture modeled in Simulink is shown in Fig. 5. A distribution system with a 25 kV 100 MVA was used and lines with a length of 21 and 2 km were used to transmit power to connected loads between busbars. A wind turbine based doubly fed induction generator was modeled and rotor side and grid side controls were performed. An indirect MPPT method was used according to wind speed and optimal torque production. A 0.4 MW PV system was modeled and synchronization control with PLL was performed. The STATCOM was added to the Point of Common Coupling (PCC) for reducing the voltage fluctuation at the end of the busbar, and reactive power compensation. The current, voltage, reactive power values at the end of busbar are firstly measured for the system without STATCOM. A STATCOM rated at 3 MVAR was incorporated into the same PCC for voltage regulation. In the hybrid system with STATCOM, a variable load between 1 MVA and 5.2 MVA was employed at the end of the line. The STATCOM system is programmed at 1.077 p.u. to keep the reference voltage at 1 p.u.

In this study, the time domain criterion is used to evaluate the PI controller in the STATCOM's control circuit for voltage stability. In the control system, if the controller tuning constants get improper value, the system's characteristics may deteriorate and the system may become unstable [18]. For this reason, optimal adjustment of controller parameters and proper selection of tuning constants have an important role in the superior performance of this control.

The most common performance criterion is Integral Time Absolute Error (ITAE). The disadvantage of the Integral Absolute Error (IAE) and Integral Square Error (ISE) criteria is that while the minimization process is relatively low, the transient response is bad. This disadvantage is addressed by using ITAE or Integral Time Square Error (ITSE) [20]. In this study, ITAE performance criterion is used as objective function for optimization.

2.4. GA based method

Genetic programming solves problems by applying three steps: Step 1. Identification of fitness function. Step 2. Coding (genetic coding). Step 3. Selecting the starting population to be random individuals. Repetition is performed until a sufficiently good

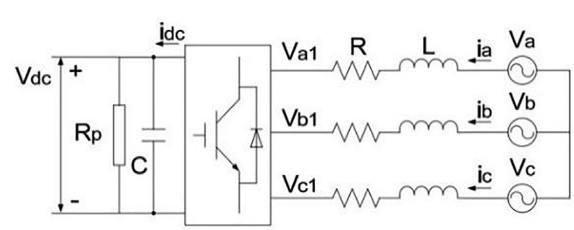

Fig. 3. The equivalent circuit of STATCOM.

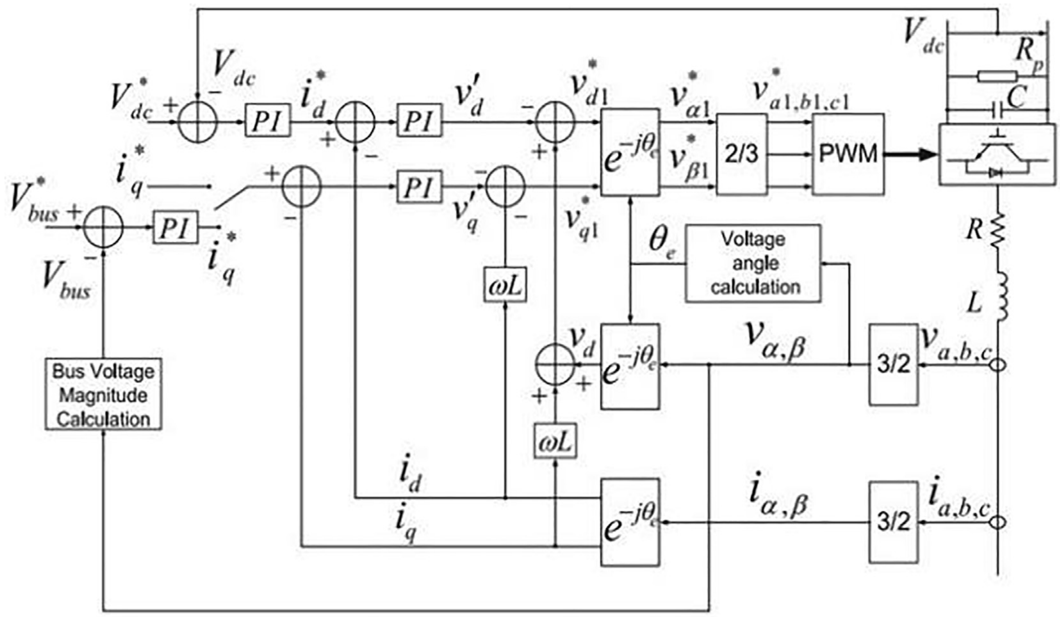

Fig. 4. STATCOM control circuit [19].

Table 1
System parameters of STATCOM model.

Parameter	Numerical Value
Grid line voltage	25 kV
Equivalent resistor	0.0012 Ω
Equivalent inductor	1.2 mH
Shunt capacitor	1600 μF
Capacitor voltage	2400 V
System frequency	60 Hz

solution is found and the fitness function of all individuals in the population is computed. The best individuals are chosen for the new generation and crossover and mutation are used to create a new generation. The new generation (chromosomes) is added to the population and the best solution is found. Optimization techniques such as GA and BFA are applied to optimize K_p and K_i gain parameters for STATCOM according to ITAE as an objective function. The flow diagram in Fig. 6 shows the steps used to optimize the K_p and K_i gain constants for STATCOM based on GA.

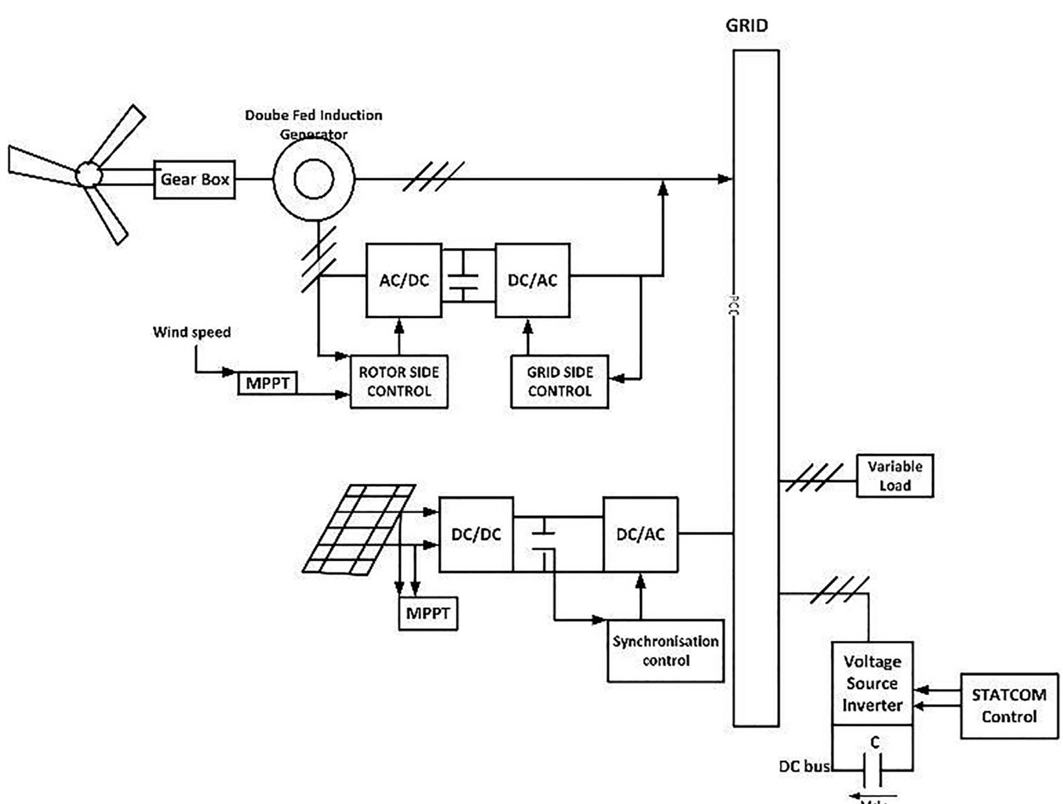

Fig. 5. Solar-Wind Hybrid System including STATCOM.

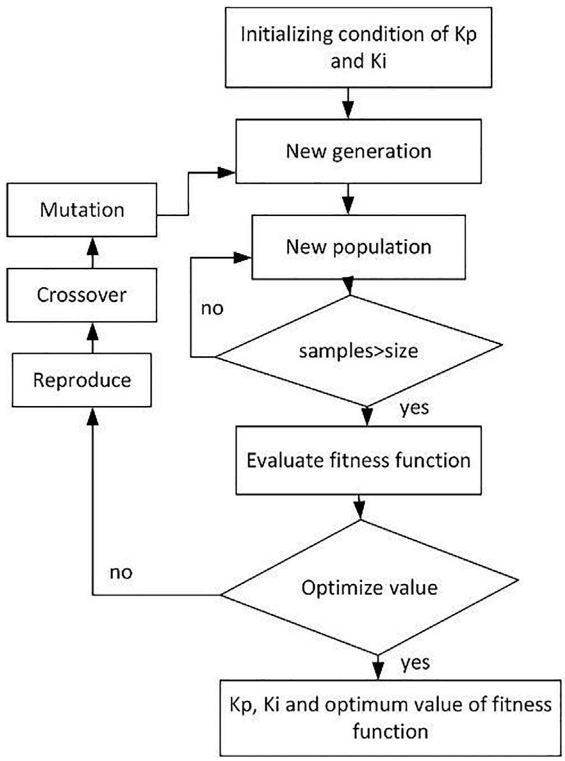

Fig. 6. Flow diagram for STATCOM tuning using GA.

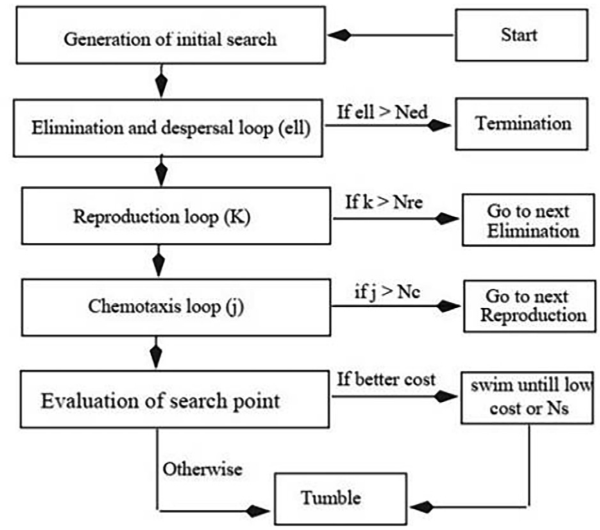

Fig. 7. Flow diagram for STATCOM tuning using BFA.

2.5. BFA based method

The bacterium E coli is based on a control system that allows to seek for food and try to evade harmful substances. The movement of bacteria can be modelled in four steps: Step 1. Swarming and Tumbling via flagella (N_s); Bacteria swims a number of N_s or less steps based on the nutrition concentration. Each flagellum operates relatively independent of the others, and the Tumbling mode specifies whether the direction of swimming changes in the future. Step 2. A chemotaxis step (N_c) gives the m swimming step followed by a tumble. N_{ed} is number of elimination and dispersal steps. A randomly determined length vector with a delta (n, i) direction to represent a tumble is generated. i is the bacterial index with the maximum bacterial s number. This step is necessary to determine the movement direction after a tumble. The position of each bacterium is indicated and the new bacterium position is given after rolling. Step 3. After N_c chemotactic steps, a reproduction step (k) is determined and the number of breeding steps is called N_{re}. Most unhealthy bacteria die and then the healthiest bacteria are divided into two bacteria, each of which is placed in the same area. Step 4. Elimination can occur when significant local increases in temperature kill a population of bacteria in a highly nutritious place. It also has the effect of helping Chemotaxis, because it can place dispersal bacteria near abundant sources of food. The flow diagram in Fig. 7 shows the steps to optimize the value of the K_p and K_i gain constants using BFA for STATCOM.

2.6. Formulation of the objective function

In this paper, as the objective function ITAE is adopted and performance criterion for optimization is called 'J'. The ITAE function is shown in Eq. (11).

$$J_{ITAE} = \int_0^T |(error)|td(t) \tag{11}$$

here T, which is the upper limit of the integral, is generally determined as larger than settling time for which integral tends to a steady state value. The sum of the errors in the control circuit of the STATCOM in Eq. (12) is considered to be the objective function.

$$OF(X) = w\int_0^T |e_{ac}|td(t) + \int_0^T |e_{dc}|td(t) + \int_0^T |e_{iq}|td(t) + \int_0^T |e_{id}|td(t) \tag{12}$$

where, $X = [K_{p1}\ K_{i1}\ K_{p2}\ K_{i2}\ K_{p3}\ Ki_3\ K_{p4}\ K_{i4}]$ and w represents the weighting factor. Eq. (12) is used for regulating DC voltage controller, AC voltage controller, current controller (I_d, I_q) and for optimization, the STATCOM's control circuit is configured as shown in Fig. 8. The total error value is calculated according to ITAE formulation in Simulink and is optimized according to ITAE formulation. GA and BFA codes, which are compatible with the m-function code file have been written, and a good optimization has been carried out with the correct restriction, multiplication, mutation and population size values. The m-function file programmed in MatLab optimize eight variables, optimization is done in eight-dimensional search space and K_p and K_i values are determined according to certain lower and upper limits.

3. Simulation results and discussion

Depending on the connection of the solar PV and wind power plants to the grid, the impact of distribution networks on the power quality increases [4]. These power quality problems caused by renewable sources are usually slow voltage variations, voltage collapses, rapid voltage changes, harmonics, and frequency imbalances. One of the most striking problems in the adoption of the solar PV and wind power systems to the network is the voltage fluctuations. The voltage fluctuation has been minimized by STATCOM's control scheme and the voltage profile improvement and reactive power compensation has been done by STATCOM.

3.1. Simulation results of STATCOM for power factor compensation

When the system is tested, the magnitude of voltage source was increased by 0.2 s as reflected in Fig. 9(a). Reference current and reactive current components that decrease in inductive mode and increase in capacitive mode is shown in Fig. 9(b). STATCOM compensated this voltage by absorbing +2.7 MVAR of reactive power.

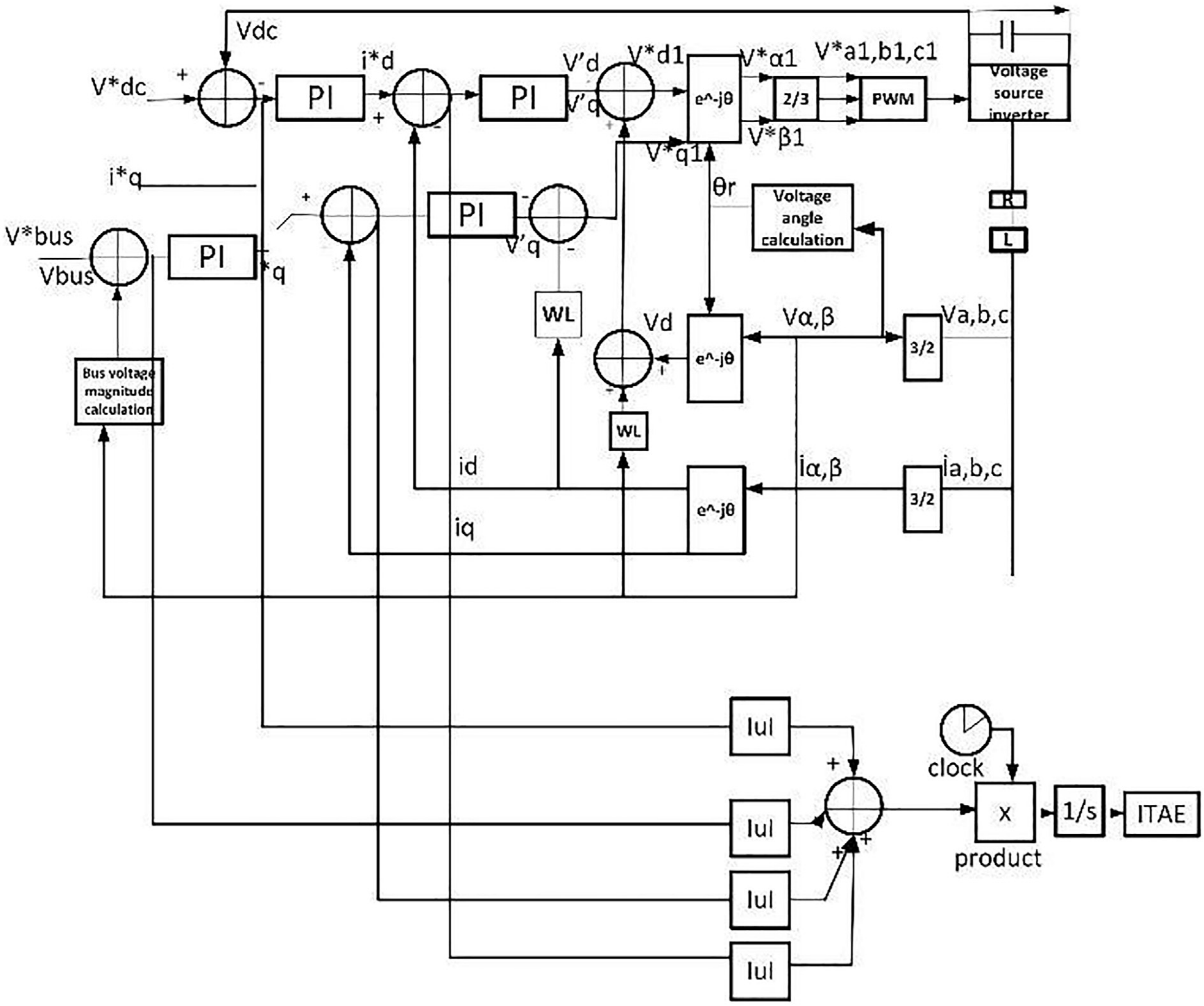

Fig 8. Control circuit of STATCOM for ITAE.

The magnitude of voltage source was reduced at 0.3 s and STATCOM produced reactive power while maintaining the voltage value by changing the reactive power from +2.7 to −2.7 MVAR as shown in Fig. 9(c). As shown in Fig. 9(d), DC voltage is tried to be kept constant and the modulation index is referred in Fig. 9(e). STATCOM operates in inductive mode beginning from 0.2 s ($m_a = 0.65$), whereas at 0.3 s in capacitive mode ($m_a = 0.85$), in which reactive power is generated. The simulations were carried out for a time period of 0.5 s.

3.2. Simulation results of solar-wind hybrid system with STATCOM for reactive power compensation

The hybrid micro-grid system firstly operates without STATCOM incorporation, and it can be reflected in Fig. 10(a) that at the end of the busbar, the voltage value increases to 1.08 p.u. at 0.2 s and decreases to 0.92 p.u. at 0.3 s. A voltage fluctuation between ±10% can be clearly seen. In the hybrid system incorporating STATCOM, the voltage is kept constant at 1.0 p.u. at all points in Fig. 10(b), and the fluctuation between 0.2 and 0.4 s. is reduced by 8% for conventional PI controller. The result of the optimization is the voltage profile at the end of the busbar in Fig. 10(b). In Fig. 10 (b), the graphs for the ITAE performance criterion show that the PI controller has the highest overshoot and peaks at some points, the voltage profiles of the GA reaches a point of 1 p.u. at 0.05 s and have a lower overshoot and the voltage fluctuation is minimized. When BFA is applied, the voltage profile reaches 1 p.u. at 0.02 s, it has the lowest overshoot and is at 1 p.u. at all points. The voltage fluctuation is reduced by 10% for GA-based PI controller, and by 15% for BFA-based PI controller. In the result of three methods, comparisons can be made in terms of voltage fluctuations and the method of adjusting the system parameters as voltage response. The optimization algorithms were run several times and the best values chosen are listed in Table 2. The results show that optimal adjustment of controller parameters and proper selection of tuning constants have vital role in controlling performance.

4. Conclusions

In this study, the impacts of a 2 MW wind power induction generator based wind generation system and a 0.4 MW solar power generation system on the grid were investigated. For this hybrid system, it has been pointed out that STATCOM provides reactive power compensation. A solar PV-wind power system with a hybrid structure was designed and the voltage profiles at the output were examined. STATCOM was incorporated to study the voltage profiles in the system according to capacitive and reactive operating states. On this basis, this work pointed out that power instability in large transmission systems can be minimized, and the fluctuations caused by the adoption of renewable energy sources to the system can be diminished.

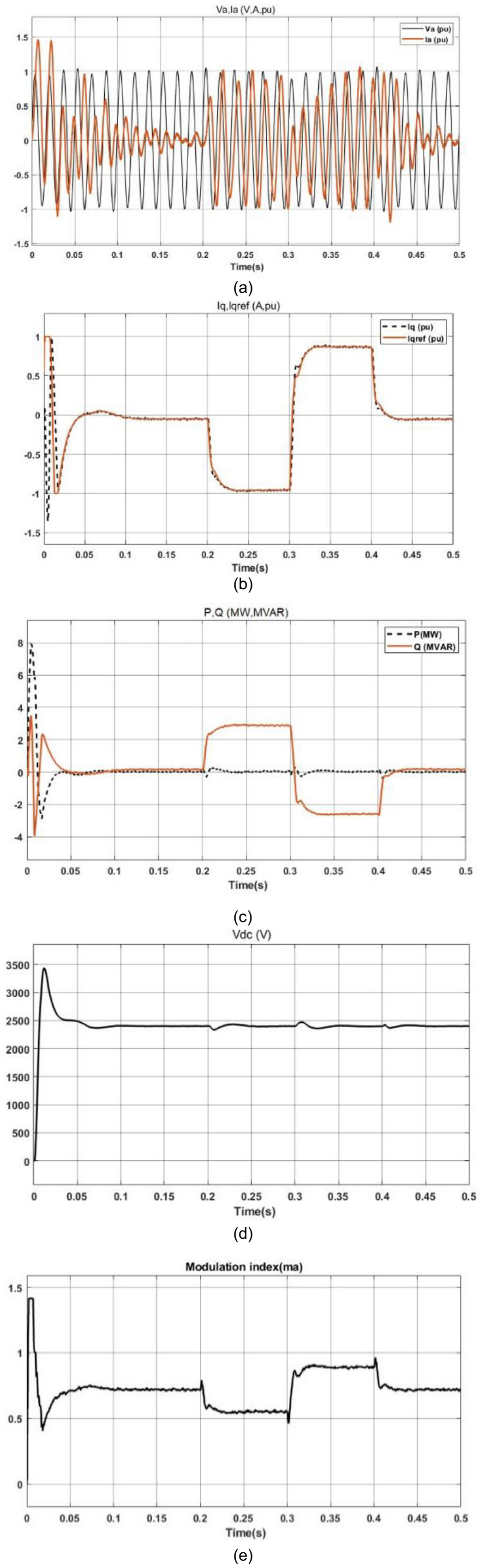

Fig. 9. (a) STATCOM output voltage profile (b) reactive current component (c) produced or absorbed active and reactive power by STATCOM (d) DC link voltage (e) modulation index waveforms.

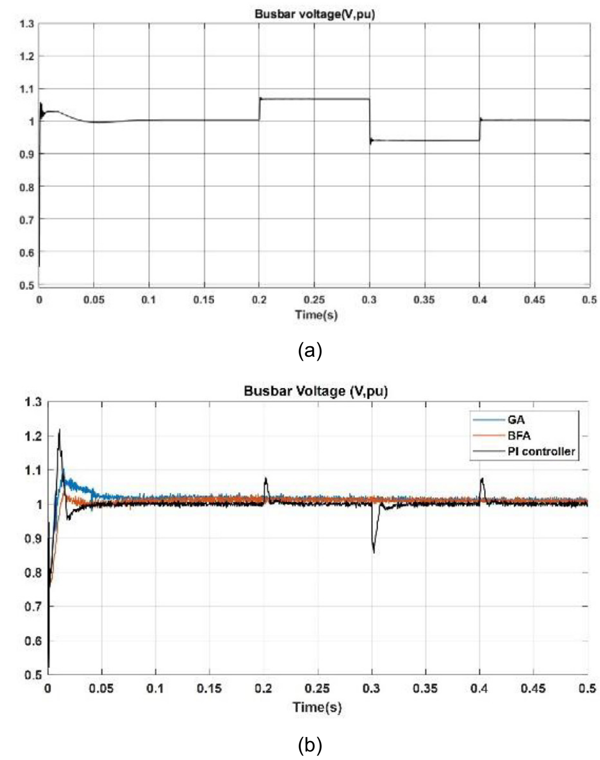

Fig. 10. (a) Voltage profile at the end of the busbar without STATCOM (b) voltage profile at the end of the busbar for conventional PI controller, GA optimized controller, BFA optimized controller with STATCOM (p.u.)

Table 2
Controller gain constants in STATCOM optimized for ITAE.

ITAE	AC regulator	DC regulator	I_d current regulator	I_q current regulator
PI constant	K_{p1} K_{i1}	K_{p2} K_{i2}	K_{p3} K_{i3}	K_{p4} K_{i4}
GA results	0.3747 0.5694	0.0114 0.8051	0.9748 0.3043	0.04292 0.7021
BFA results	0.8662 0.6752	0.2393 0.0285	0.2639 0.7486	0.4308 0.9502

The comparisons of the results showed that the effectiveness of the STATCOM tuned with GA and BFA was improved. By acquiring the best values for PI controller gains, voltage swell occurred due to the change in reactive power has been overcome and a better dynamic response was reached. In future studies, different optimization techniques and different FACTS devices can be used to compare and determine a more effective one.

References

[1] F.H. Gandoman, A. Ahmadi, A.M. Sharaf, P. Siano, J. Pou, B. Hredzak, V.G. Agelidis, Review of FACTS technologies and applications for power quality in smart grids with renewable energy systems, Renew. Sustain. Energy Rev. 82 (2018) 502–514, https://doi.org/10.1016/j.rser.2017.09.062.

[2] A. Mohanty, M. Viswavandya, D.K. Mishra, P.K. Ray, S. Pragyan, Modelling & simulation of a PV based micro grid for enhanced stability, Energy Proc. (2017) 94–101, https://doi.org/10.1016/j.egypro.2017.03.060.

[3] H. Liao, S. Abdelrahman, J.V. Milanović, Zonal mitigation of power quality using FACTS devices for provision of differentiated quality of electricity supply in networks with renewable generation, IEEE Trans. Power Deliv. 23 (2017) 1975–1985, https://doi.org/10.1109/TPWRD.2016.2585882.

[4] A. Saraswathi, P. Sanjeevikumar, S. Shanmugham, F. Blaabjerg, A.H. Ertas, V. Fedák, Analysis of enhancement in available power transfer capacity by STATCOM integrated SMES by numerical simulation studies, Eng. Sci. Technol., Int. J. 19 (2) (2016) 671–675, https://doi.org/10.1016/j.jestch.2015.10.002.
[5] D. Menniti, A. Pinnarelli, N. Sorrentino, An hybrid PV-Wind supply system with D-Statcom interface for a water-lift station, International Symposium on Power Electronics, Electrical Drives, Automation and Motion, 2010. DOI: 10.1109/SPEEDAM.2010.5545070.
[6] N.S. Kumar, J. Gokulakrishnan, Impact of FACTS controllers on the stability of power systems connected with doubly fed induction generators, Electr. Power Energy Syst. 33 (2011) 1172–1184, https://doi.org/10.1016/j.ijepes.2011.01.031.
[7] S. Li, L. Xu, T.A. Haskew, Control of VSC-based STATCOM using conventional and direct-current vector control strategies, Electr. Power Energy Syst. 45 (2013) 175–186, https://doi.org/10.1016/j.ijepes.2012.08.060.
[8] D.K. Yadav, T.S. Bhatti, Voltage control through reactive power support for WECS based hybrid power system, Electr. Power Energy Syst. 62 (2014) 507–518, https://doi.org/10.1016/j.ijepes.2014.04.067.
[9] P. Sharma, T.S. Bhatti, K.S.S.S. Ramakrishna, Control of reactive power of autonomous wind-diesel hybrid power systems, Joint International Conference on Power Electronics, Drives and Energy Systems (PEDES), 2010. DOI: 10.1109/PEDES.2010.5712461.
[10] V. Sitthidet, N. Issarachai, K. Somyot, Coordinated SVC and AVR for robust voltage control in a hybrid wind-diesel system, Energy Convers. Manage. 51 (2010) 2383–2393, https://doi.org/10.1016/j.enconman.2010.05.001.
[11] B. Abhik, V. Mukherjee, S.P. Ghoshal, Modeling and seeker optimization based simulation for intelligent reactive power control of an isolated hybrid power system, Swarm Evol. Comput. 13 (2013) 85–100, https://doi.org/10.1016/j.swevo.2013.05.003.
[12] A.A. Tanvir, A. Merabet, R. Beguenane, Real-time control of active and reactive power for doubly fed induction generator (DFIG)-based wind energy conversion system, Energies 8 (2015) 10389–10408, https://doi.org/10.3390/en80910389.
[13] S.B. Birinç, Dynamic Modeling and Comparison of Variable Speed Wind Power (Plants, Master's thesis), Yildiz Technical University, Institute of Science, 2008.
[14] G. Abad, J. López, M.A. Rodríguez, L. Marroyo, G. Iwanski, Dynamic Modeling of the Doubly Fed Induction Machine, Electronic Book, John Wiley & Sons Inc, 2011.
[15] M.A. Ozcelik, A.S. Yilmaz, S. Kucuk, M. Bayrak, Efficiency in centralized DC systems compared with distributed DC systems in photovoltaic energy conversion, Elektronika Ir Elektrotechnika 21 (6) (2015) 51–56, https://doi.org/10.5755/j01.eee.21.6.13761.
[16] E.I.A. Mahmoud, M. Maaroufi, A.K. Mahmoud, A. Yahfdhou, Optimization of Statcom in a Nouakchott power system, Adv. Sci. Technol. Eng. Syst. J. 4 (2) (2019) 333–339, https://doi.org/10.25046/aj040242.
[17] M. Karataş, Control of Static Synchronous Compensator with PID Controller (Master's thesis), Electrical and Electronics Engineering, Malatya, Turkey, 2011.
[18] M.I. Mosaad, M.O.A. El-Raouf, M.A. Al-Ahmar, F.M. Bendary, Optimal PI controller of DVR to enhance the performance of hybrid power system feeding a remote area in Egypt, Sustain. Cities Soc. 47 (2019), https://doi.org/10.1016/j.scs.2019.101469.
[19] L. Xu, Control of Power Converter for grid Integration of Renewable Energy Conversion and Statcom Systems, Master's thesis, Tuscaloosa, Alabama, 2009.
[20] A.H. Hajisalem, Optimization of PID Control Parameters for Wind /PV Solar Energy Systems with GA and PSO (Master's thesis), Karadeniz Technical University, Electrical and Electronics Engineering, Trabzon, Turkey, 2013.